Effects of Nanoclay on Cellular Morphology and Water Absorption Capacity of Poly(vinyl alcohol) Foam

Jahanmardi, Reza**+; Eslami, Behnam; Tamaddon, Hamed

Department of Polymer Engineering, Science and Research Branch, Islamic Azad University, Tehran, I.R. IRAN

ABSTRACT: *The present work was aimed to examine the effects of incorporation of each of two different types of nanoclay, i.e. Cloisite Na+ and Cloisite 30B, into PVA foam on cellular morphology and water absorption capacity. Foam samples containing 0.0-10.0 wt% of each of the two types of nanoclay alone were prepared using mechanical foaming. Accordingly, PVA/organoclay/water suspensions were prepared first. Then other agents, i.e. catalyst, surfactant and crosslinking agent were added, respectively, to each of the prepared suspensions rendering primary froths, which were converted to final foam samples at room temperature during a period of 24 h. State of clay dispersion in the polymer matrix and cellular morphology of the prepared foam samples were examined using X-Ray Diffraction (XRD) technique and Field Emission Scanning Electron Microscopy (FESEM), respectively. Also, dry foam density and water absorption of the foam samples were measured gravimetrically. XRD patterns revealed the existence of intercalated and exfoliated structures in the PVA/Cloisite 30B and the PVA/Cloisite Na+ foam samples, respectively. FESEM images demonstrated open-cell morphology for all the samples but the extent of cell wall rupture was more significant in the case of PVA/nanoclay foam samples. In addition, water absorption capacity of the PVA foam was shown to be decreased by the incorporation of either of the two types of nanoclay, which was explained in terms of the lower total pore volume in the PVA/nanoclay foam samples than in the neat PVA foam sample. Finally, the obtained results were explained in terms of the effects of the nanoparticles on the elevation of the rate of the drainage in the crosslinking PVA solution before the stabilization of the cellular structure.*

KEYWORDS: *Nanocomposite; Foam; Cellular morphology; Poly(vinyl alcohol).*

INTRODUCTION

Polymeric foams are a class of materials which contain gas bubbles surrounded by polymeric matrix. Plastic foams are known for their excellent heat and sound insulations, high strength-to-weight ratio, high energy or mass absorption, and materials saving [1-3]. So, polymer foams have diverse application in a vast area, such as, packaging, thermal insulation, acoustic attenuation, membranes for separation, absorbents and so forth [4-6]. Foams of high porosity with interconnected pores have also been used as tissue engineering scaffolds

** To whom correspondence should be addressed.*
+ E-mail: r.jahanmardi@srbiau.ac.ir
1021-9986/2017/4/59-67 *9/$/5.90*

for cell attachment and growth [7]. Polymer foams can be defined as either closed cell or open cell foams. In closed cell foams, the foam cells are isolated from each other and cavities are surrounded by complete cell walls. In open cell foams, there is not certain wall between cells and the structure is conjunct. Generally, closed cell foams have lower permeability, leading to better insulation properties. Open cell foams, on the other hand, provide better absorptive capability.

Poly(vinyl alcohol) (PVA) foams are rigid open-cell foams that exhibit good mechanical properties at relatively low densities (0.02-0.2 g/cm^3) [8, 9]. Their unique properties, i. e., abrasion resistance, resiliency, high water absorption capacity and chemical stability, make them excellent choice for various applications, such as, washcloths, mops and surgical pads. These properties make PVA foamed composites a good candidate for surgical implants and dressings [10,11]. The wet foams make excellent dressings for burns, since they protect the wound while keeping the area irrigated and allowing air to pass into the wound. However, the open-cell structure and hydrophilic nature of PVA foam restricts its use in both construction and packaging. Furthermore, the foams have the capacity to accept large quantities of filler (800-1200%wt) without big change in their original properties.

Besides, nanocomposites are a new class of materials providing superior properties compared to their micro composite counterparts. Nanocomposites usually refer to composites in which at least one phase (the filler phase) possesses ultrafine dimensions (on the order of a few nanometers). An addition of a small amount of nanoparticles can significantly improve a variety of properties without sacrificing the lightweight of polymer matrices [12-14]. The combination of functional nanofillers and foaming technology has a high potential to generate a new class of materials that are light, strong, and multifunctional [15]. Hence, in recent years, polymer nanocomposite foams have received increasing attention in both the scientific and industrial community [16, 17]. Nanocomposite foams have a high position and vast area of applications, such as aerospace, automotive, packaging and home appliances.

Low density is one of the most attractive properties of polymer foams as a light weight substitute for structural or functional materials. However, the polymer foams' mechanical properties are almost always compromised after density reduction [18]. A combination of light weight and high strength has always been the major research objective in the research area of polymer foams. The physical and mechanical properties of polymer foams not only depend on the intrinsic properties of the polymer, but also on the microstructure of the foam, such as cell density, cell size and cell size distribution.

The present study was carried out in order to examine the capability of nanoclay in enhancement of water absorption capacity of PVA foams. Hence, we tried to prepare PVA/nanoclay nanocomposite foams, for the first time. Then, effects of incorporation of two different types of nanoclay, i.e., Cloisite Na^+ and Cloisite 30B, into PVA foams on cellular morphology and water absorption capacity of the foams were investigated.

EXPEIMENTAL SECTION

Materials

In this study, poly(vinyl alcohol) with average molecular weight of 72 kDa and hydrolysis degree of 99% was purchased from Merck Chemical Co. Two types of montmorillonite clay including sodium containing natural montmorillonite (with trade name of Cloisite Na^+) and organically modified nanonoclay (with trade name of Cloisite 30B) from Southern Clay Products Inc. were used. Cloisite Na^+ had Cation Exchange Capacity (CEC) of 92.6 meq per 100 g of clay and amount of clay surface modification in Cloisite 30B was equal to 90 meq per 100 g clay. Formaldehyde in the form of 37% aqueous solution from Sigma-Aldrich Chemical Co., polysorbate 20 from Sino-Japan Chemical Co. and sulfuric acid (98% aqueous solution) and sodium hydroxide from Merck Chemical Co. were used as received.

Synthesis of poly(vinyl alcohol) nanocomposite foams

Nanocomposite foams containing 0.0-10.0 wt% of each of the two types of nanoclay alone were prepared according to the following procedure: Firstly, fine organoclay/water suspensions were prepared through stirring for 2.5 h at 6000 rpm followed by sonication for 15 minutes. Each of the prepared suspensions was then combined with a certain amount of PVA/water solution and stirred to render a homogeneous suspension in which the final concentration of the polymer was 10% by weight. Each of the aqueous PVA/clay suspensions was then sonicated for an extra 15 minutes. Certain amounts

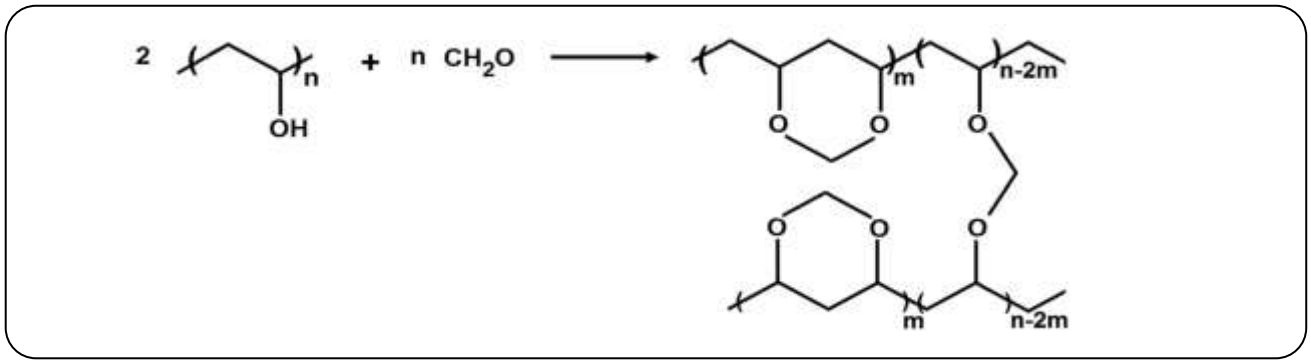

Scheme 1: Crosslinking and acetalization reactions of poly(vinyl alcohol) with formaldehyde [19].

of sulfuric acid solution (65%) were then mixed with each suspension so that the final concentration of the acid became 14% by weight. Then each prepared suspension was poured into a plastic vessel equipped with a rotary beater and was mixed with certain amount of polysorbate 20 (i. e., 50% by weight of the polymer in the suspension) and the beater was increased to its highest speed (1000 rpm) until an equilibrium maximum froth volume was reached. The aqueous solution of formaldehyde was then added to the froth and let to be mixed for two minutes more. The amount of formaldehyde used was 51% by weight of the polymer which was 50% more than its stoichiometric ratio to the polymer in the crosslinking reaction of the polymer according to Scheme 1 [19]. The froth was then poured into a plastic mold and kept at room temperature for a period of 24 hours after which the cured foam was washed with NaOH solution in order to neutralize the residual acid and formaldehyde. The procedure is illustrated schematically in Scheme 2. Also, sample designation and formulation of the prepared foam samples are given in Table 1.

Measurements and characterizations

The interlayer spacing of the organoclays was measured by X-Ray Diffraction (XRD) technique using a X' Pert MPD model Philips instrument equipped with Cu radiation source at 40 kV, 30 mA, λ = 0.1542 nm, 2θ ranging between 2 and 10° and imaging speed of 0.01 s^{-1}. The peak position in the spectrum (2θ) and the Bragg equation as it is shown in equation (1) were used to calculate distances between clay layers:

$$n\lambda = 2d\sin\theta \quad (1)$$

where, n is an integer, λ is the wavelength of X-ray beam (0.1542 nm), and d is the interplanar spacing of the organoclay crystals.

The morphology of the prepared poly(vinyl alcohol) foams was observed by field emission scanning electron microscopy (FESEM) using a Leo 440i unit. Specimens for FESEM were freeze-fractured in liquid nitrogen and the fracture surface was sputter-coated with gold in argon plasma for 3 min. Images were obtained using 15kV accelerating voltage.

Water absorption capacity of the prepared foams was measured according to ASTM C272. Firstly, five 75×75×12 mm^3 cubic specimens were cut from each foam sample. Then the specimens were dried in an oven, allowed to cool in a desiccator and then were weighed on an analytical balance to the nearest 0.01 g. The specimens then were immersed in deionized water to a depth of 50 mm and were removed from the water after 24 hours. The specimens were weighed immediately after that all surface water was wiped off with a dry cloth. Water absorption capacity was defined as the maximum amount of water absorbed by dry foam and was expressed as wt% of the dry foam.

In order to determine dry foam density, prepared foams were dried and cut into small cubes using a chain saw. Dimensions and weight of each cube were precisely measured and the cube density was simply calculated by dividing the cube weight to its own volume. The dry density of each foam sample was expressed as the average of at least five cubic specimens.

RESULTS AND DISCUSSION

State of clay dispersion in the prepared nanocomposites foams

XRD technique has been extensively used for determination of the gallery height (d-spacing distance) in clay stacked particles [20]. XRD patterns of neat Cloisite 30B and PVA/C5 foam sample containing 5 wt% of

Table 1: Formulation of the prepared PVA foam samples.

Sample designation	Cliosite 30B (wt %)	Cloisite Na+-MMT (wt %)
PVA	0.0 (neat poly(vinyl alcohol) foam)	0.0
PVA/C1	1.0	-
PVA/C2	2.0	-
PVA/C5	5.0	-
PVA/C10	10.0	-
PVA/N1	-	1.0
PVA/N2	-	2.0
PVA/N5	-	5.0
PVA/N10	-	10.0

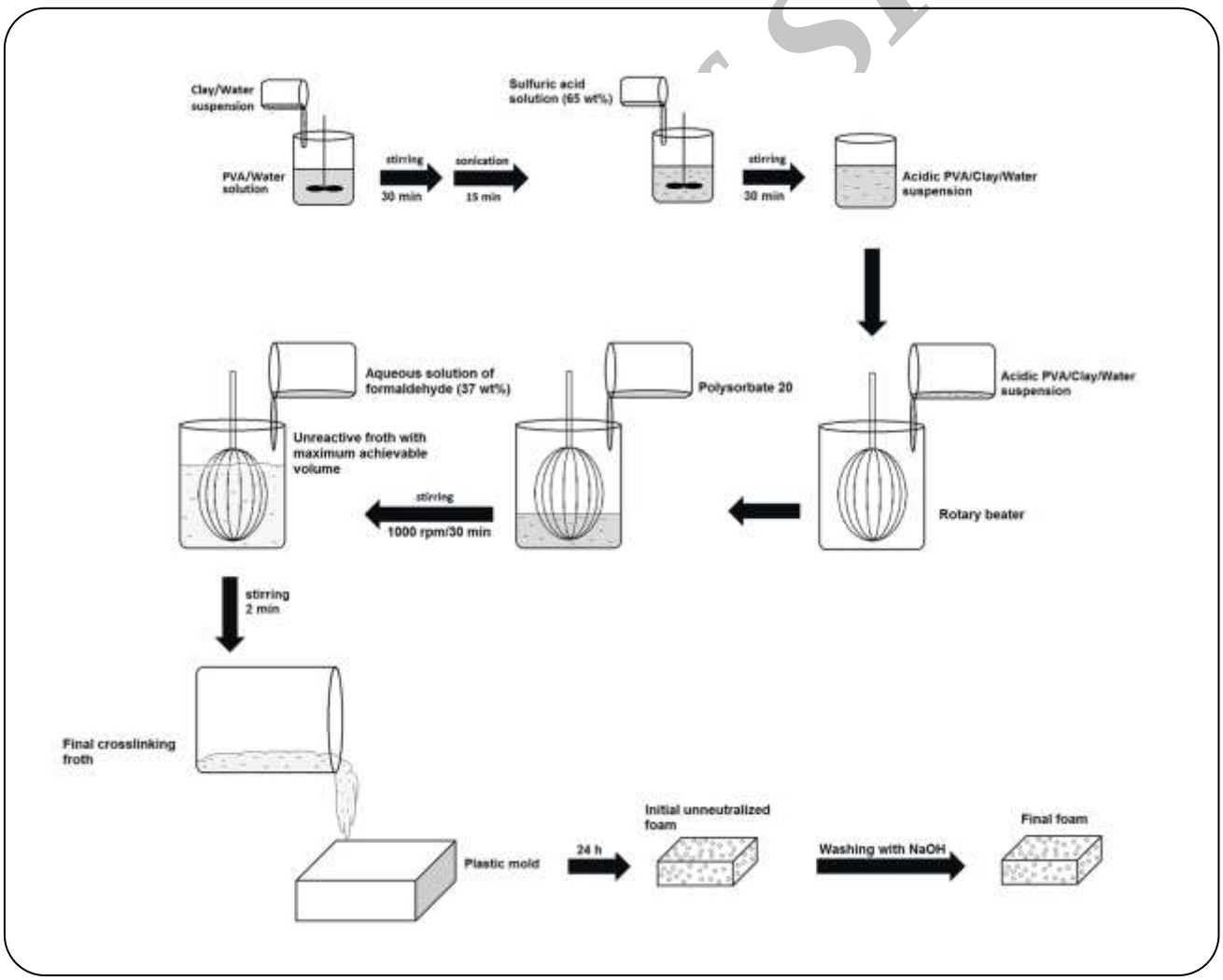

Scheme 2: A schematic representation for the procedure of the preparation of the nanocomposites foam samples.

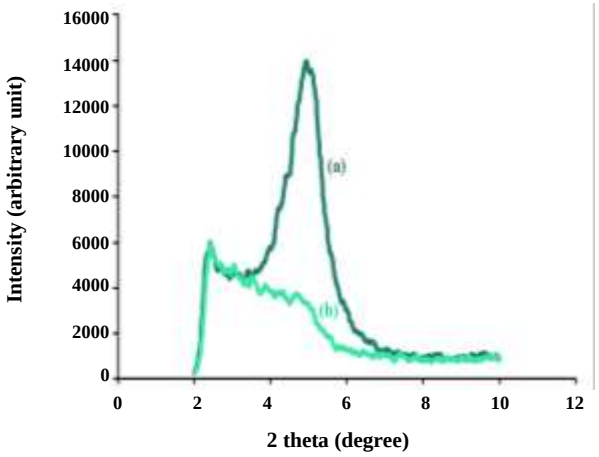

Fig. 1: XRD patterns of (a) neat Cloisite 30B nanoclay and, (b) PVA/C5 foam sample.

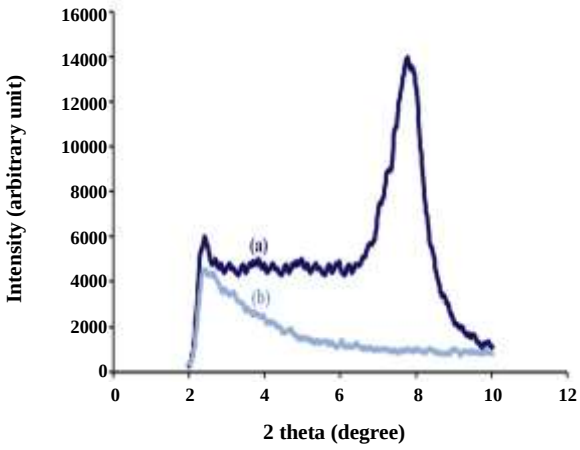

Fig. 2: XRD patterns of (a) neat Cloisite Na^+ nanoclay and, (b) PVA/N5 foam sample.

Cloisite 30B are shown in Fig. 1. As it is seen in the figure, Cloisite 30B powder shows a diffraction peak at a 2θ angle of 4.86° which is corresponding to a d-spacing of 1.82 nm according to the Bragg equation. On the other hand, the diffraction peak of the nanoclay in the PVA/C5 foam sample has been weakened significantly and the peak position has been shifted to 2θ angle of 4.46°. This indicates the formation of intercalated structures of Cloisite 30B in which the d-spacing of the clay platelets has been increased to 1.98 nm. Also, XRD patterns of neat Cloisite Na+ and PVA/N5 foam sample containing 5 wt% of Cloisite Na+ are shown in Fig. 2. It is seen that Cloisite Na+ exhibits a diffraction peak at a 2θ angle of 7.71°, which corresponds to a d-spacing of 1.15 nm. It should be mentioned that the calculated d-spacing of both Cloisite 30B and Cloisite Na+ are in close agreement with the d-spacing values of 1.85 nm and 1.17 nm, respectively, provided by the supplier. Moreover, no diffraction peak is seen for Cloisite Na+ in the XRD pattern of the PVA/N5 foam sample that could be attributed to the exfoliation of the stacked structure of the nanoclay. It could be concluded that as Cloisite Na+ nanoclay has higher surface polarity, compared to Cloisite 30B, interactions between the polar polymer chains and surfaces of the nanoclay particles in the PVA/Cloisite Na+ nanocomposite foam sample are stronger than those in the PVA/Cloisite 30B nanocomposite foam sample [21]. So, the more compatibility between the polymer and the nanoparticles in the PVA/Cloisite Na+ nanocomposite foam leads to a better state of dispersion in this nanocomposite in comparison to that in the PVA/Cloisite 30B nanocomposite foam.

Water absorption capacity and dry bulk density of the prepared foams

One of the most important features of PVA foams is their high water absorption capacity. So, water absorption capacity of the prepared foams was measured in this work and the obtained data is presented in Fig. 3. As it is seen in Fig. 3, the incorporation of each of the two types of nanoclay into PVA foam results in a significant decrease in water absorption capacity of the prepared PVA foams and the amount of the diminution is proportional to the concentration of the nanoclay in the foam sample. As water is absorbed to the hydrophilic surface of cell walls of PVA foam, it could be expected that water absorption capacity of PVA foam depends on its overall surface of cell walls. In addition, the overall surface of cell walls in a PVA foam is dependent on its total pore volume which, in turn, is inversely proportional to its dry bulk density. Accordingly, dry bulk density of all the prepared PVA foam samples was measured in order to examine the above elucidation. The obtained data is illustrated in Fig. 4. As it is seen in in Fig. 4, dry bulk density is increased by the incorporation of each type of nanoclay alone and the amount of the enhancement of the density is proportional to the concentration of the nanoclay in the foam sample. Therefore, this observation justifies the above explanation. Accordingly, it could be concluded that the

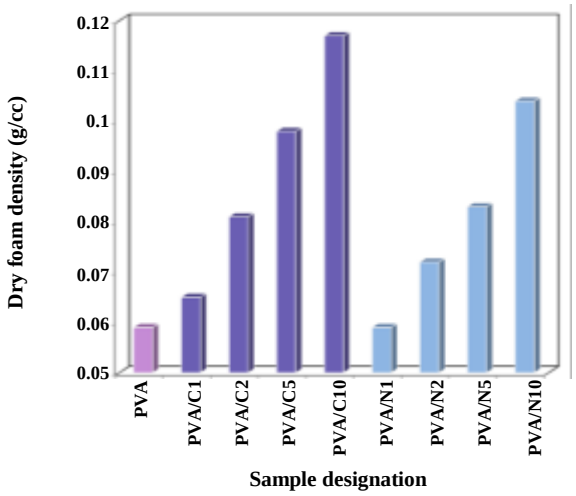

Fig. 3: Water absorption capacity of the prepared PVA foam samples.

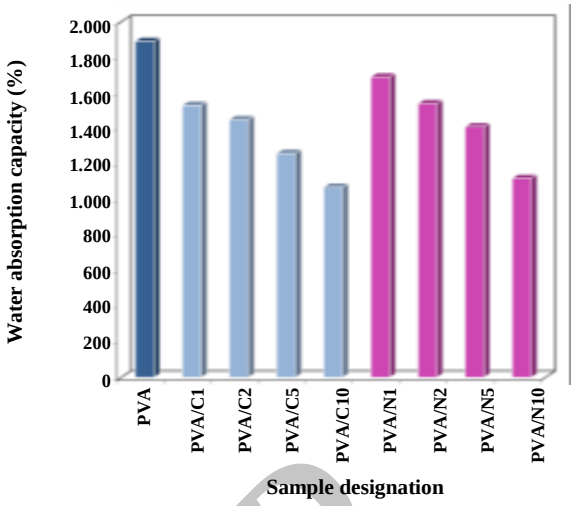

Fig. 4: Dry bulk density of the prepared PVA foam samples.

incorporation of nanoclay into the PVA foam samples decreases their expansion ratio and their total pore volume, which, in turn, results in the enhancement of their dry bulk density. Moreover, the data presented in Figs. 3 and 4 suggest that each PVA foam sample containing Cloisite Na+ has slightly higher water absorption capacity and relatively lower dry foam density in comparison with the PVA foam sample containing the same concentration of Cloisite 30B. This observation is in agreement with the above explanation. However, finding a reason for the different expansion ratios obtained by the incorporation of the same amount of each of the two different types of nanoclay alone requires evaluation of the cellular morphology of the prepared foam samples which will be presented in the following section.

Cellular morphology of the prepared foam samples

In order to find a reason for the observed effects of the incorporation of each of the nanoclays on expansion ratio of the prepared PVA foam samples, cellular morphology of the foams was studied by using FESEM. FESEM images of neat PVA foam sample and the PVA/C1 sample containing 1% by weight of Cloisite 30B and the PVA/N1 sample containing 1% by weight of Cloisite Na+, respectively, are illustrated in Fig. 5, with three different magnification factors. In images a-1, b-1 and c-1of Fig. 5, which have the lowest magnification factor among the other images of the figure, open-cell morphology is seen for all the three samples, which is a general phenomenon for poly(vinyl alcohol) foams [8, 9]. This is due to the fact that all liquid foams (froths) are thermodynamically unstable because of their higher surface free energy in comparison with their initial segregated gas and liquid forms. Thus, all liquid foams have a tendency to reduce their free energy via collapse of foamed structure, which in turn, takes place gradually through drainage and thinning and rupture of cell walls. Another driving force for thinning of cell walls and drainage is gravitational forces. The phenomenon could be detected in practice when a mold is filled with a crosslinking PVA froth. After a time a liquid layer appears at the bottom of the mold, which contains water, unreacted PVA, formaldehyde, acid and surfactant. The liquid layer rises until the foam has crosslinked and its cellular structure has been stabilized. On the other hand, crosslinking reaction of PVA foam prevents drainage and hence, rupture of cell walls through increasing elasticity, strength and insolubility of cell walls. Therefore, one can expect that the final morphology of PVA foam is controlled by the competition between two factors: first, the rate of drainage which depends on the surface tension and the viscosity of PVA solution, and second, the rate of crosslinking which is dependent on the concentration of PVA resin, acid catalyst and formaldehyde. In the case of the formulations used in our work which is similar to the formulation used for the production of most commercial PVA foams, the competition led to the observed open-cell structure.

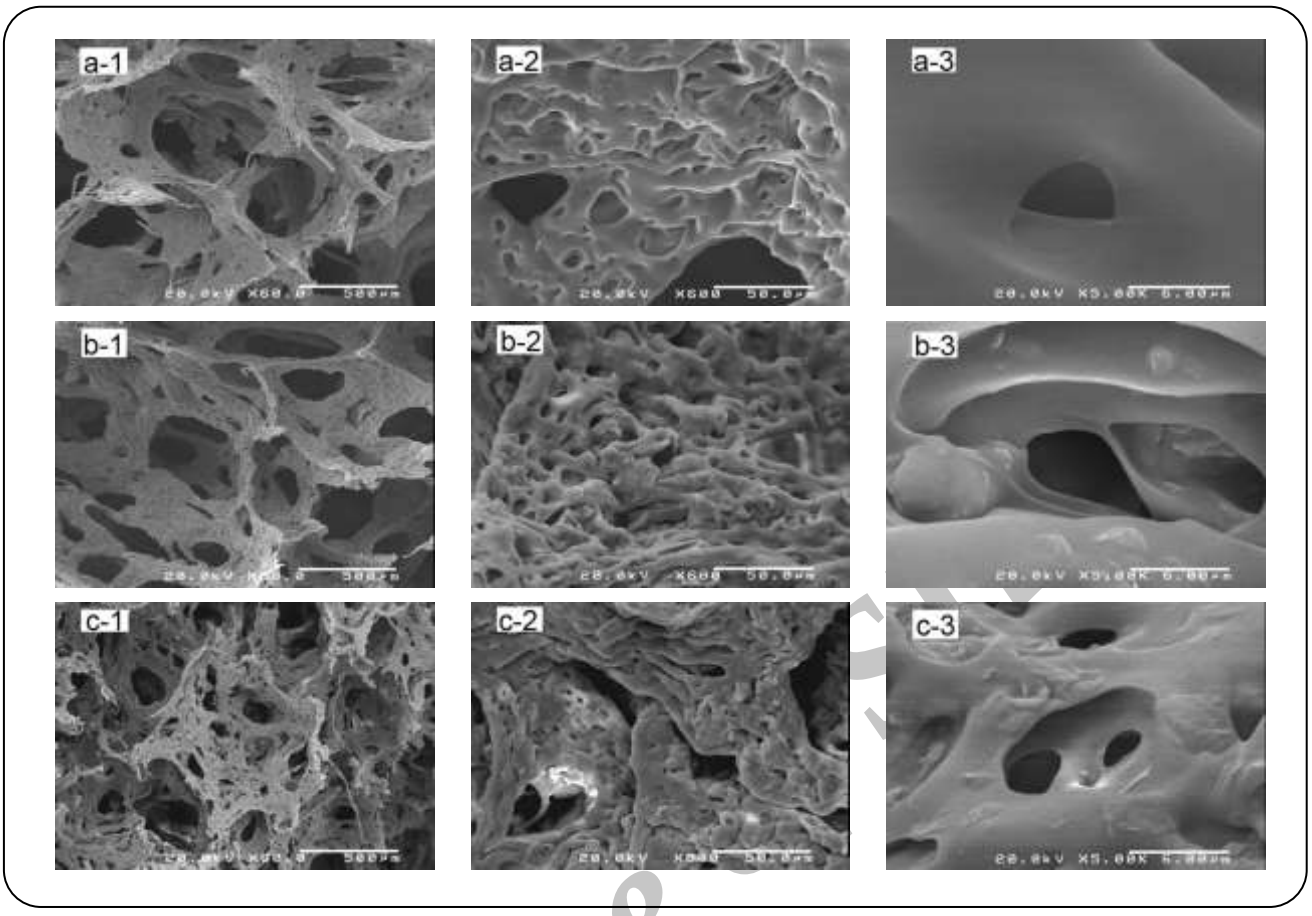

Fig. 5: FESEM images of (a-1 to a-3) PVA, (b-1 to b-3) PVA/C1 and (c-1 to c-3) PVA/ N1 foam samples with three different magnifications. Magnification factors are specified at the bottom of the images.

In addition, through comparison of the images a-2, b-2 and c-2 of Fig. 5, it could be deduced that the local collapse of the cellular structure is more pronounced in the nanocomposite foam samples. Moreover, by comparing images a-3, b-3 and c-3 of Fig. 5, which have higher magnification factor and hence, could show more details about the cell walls, one can infer that the rupture of cell walls has occurred more severely in the PVA/C1 and the PVA/N1 samples than in the PVA sample. This phenomenon could be ascribed to the following two reasons: First, increase of density of the foaming solution by the incorporation of nanoclay which in turn, enhances the rate of the drainage before the stabilization of the foam structure, and second, that the nanoclay platelets may act as shields which obstruct the formation of crosslinks between adjacent poly(vinyl alcohol) chains according to Scheme 3, and hence, delay the stabilization of the cellular structure. A similar role for nanoclay platelets in polyurethane foams was mentioned by *Lee et al.* [15]. However, it should be noted here that the proposed mechanism is elementary and additional analytical experiments is required to prove it. As a whole, one can conclude that the incorporation of each one of the two types of nanoclay into the PVA foam leads to more intense collapse of the cellular structure, which in turn, results in higher dry density and lower water absorption capacity of the foam samples.

Moreover, through comparison of the images b-2 and c-2 of Fig. 5, one can infer that the local collapse of the cellular structure of PVA/C1 sample is rather more significant than that of the PVA/N1 sample. This could be due to the better state of dispersion of Cloisite Na+ than that of Cloisite 30B in PVA matrix. Accordingly, the existence of finer nanoparticles in the PVA matrix causes less interference in the crosslinking reactions between their adjacent poly(vinyl alcohol) chains as well as lighter cell walls, which in turn, result in the lower rate of drainage and the lower amount of local structural collapse.

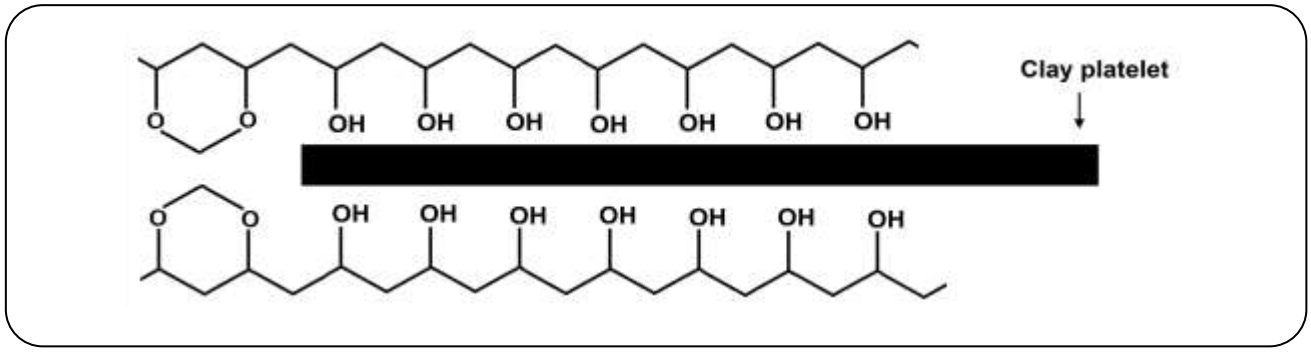

Scheme 3: The interference of nanoclay platelets in crosslinking reaction between their adjacent poly(vinyl alcohol) chains.

Eventually, it is expected that in comparison with the PVA foam samples containing Cloisite 30B, the PVA foam samples containing the same amount of Cloisite Na+ have lower dry foam density, an observation which was mentioned earlier in the text.

CONCLUSIONS

In this study, for the first time poly(vinyl alcohol)/nanoclay nanocomposite foams containing various concentrations of each of Cloisite 30B and Cloisite Na+ alone were prepared. XRD patterns of the prepared foam samples demonstrated the existence of intercalated and exfoliated structures in the PVA/Cloisite 30B and the PVA/Cloisite Na+ foam samples, respectively. The better state of dispersion in the PVA/Cloisite Na+ samples was attributed to the stronger polymer-filler interaction in theses samples in comparison with that in the PVA/Cloisite 30B samples. FESEM images taken from the prepared foam samples revealed the open-cell morphology for all the samples. However, the incorporation of each of the two types of nanoclay alone into the PVA foam was shown to enhance the extent of cell wall rupture and local collapse of the cellular structure. This was explained in terms of the effects of nanoparticles on elevation of the rate of the drainage in the crosslinking PVA solution before the stabilization of the cellular structure. Furthermore, less local structural collapse was observed in the PVA/Cloisite Na+ samples than in the PVA/Cloisite 30B samples, which was attributed to the slower rate of the drainage and less interference in the crosslinking reactions, due to the existence of finer particles in the PVA/Cloisite Na+ sample. It was also showed that the incorporation of nanoclay into PVA matrix increases dry foam density of the final foam, which is due to the more extent of the local structural collapse in PVA/nanoclay foam than in the neat PVA foam. In addition, water absorption capacity of the PVA foam was shown to be decreased by the incorporation of nanoclay. This observation was explained in terms of the lower total pore volume in the PVA/nanoclay foams than in the neat PVA foam, which is again a result of the higher amount of the local structural collapse in the PVA/nanoclay foams than in the neat PVA foam.

Acknowledgement

The authors would like to thank Mr. Mahdi Mohammadizade for his help in drafting the manuscript and Mr. Mohammad-Sadegh Amani for his help in carrying out the experiments.

Received : Jun. 10, 2016 ; Accepted : Dec. 26, 2016

REFERENCES

[1] Khosrowshahi S.M., Abbasi F., Harasi N., Maher B.M., Relationships Between Synthesis Parameters and Properties of Water Expandable Polystyrene, *J. Cell. Plast.*, **49**(1): 13-31 (2013).

[2] Liu P.S., Chen G.F., "Porous Materials Processing and Applications", Elsevier, Butterworth-Heinemann (2014).

[3] Mittal V., "Polymer Nanocomposite Foams", CRC Press, Boca Raton (2013).

[4] Lee S.T., Scholz D.P.K., "Polymeric Foams: Technology and Developments in Regulation Process", CRC Press, Boca Raton (2008).

[5] Hu X., Wouterson E.M., Liu M., "Handbook of Manufacturing Engineering and Technology", Springer, London (2014).

[6] Lobos J., Velankar S., How Much do Nanoparticle Fillers Improve the Modulus and Strength of Polymer Foams?, *J. Cell. Plast.*, **52**(1): 57-88 (2016).

[7] Mikos A.G., Temenoff J.S., Formation of Highly Porous Biodegradable Scaffolds for Tissue Engineering, *Electronic Journal of Biotechnology*, **3**: 2 (2000).

[8] Rosenblatt S., Injection molded PVA Sponge, *U.S. Pat. US5554659* (1996).

[9] Chen G., Yang X., Polyvinyl Acetate Sponge and Method for Producing Same, *U.S. Pat. US20030046783* (2003).

[10] Baia X., Ye, Z.F., Lia Y.F., Zhou L.C., Yang L.Q., Preparation of Crosslinked Macroporous PVA Foam Carrier for Immobilization of Microorganisms, *Process Biochem.*, **45**(1): 60-66 (2010).

[11] John, D.B., Lemley T.J., Petrochko C.N., Polyvinyl Alcohol Foam Particle Sizes and Concentrations Injectable Through Microcatheters, *J. Vasc. Interv. Radiol.*, **9**(1): 113-118 (1998).

[12] Faghihian H., Rasekh M., Removal of Chromate from Aqueous Solution by a Novel Clinoptilolite-Polyanillin Composite, *Iran. J. Chem. Chem. Eng. (IJCCE)*, **33**(1): 45–51 (2014).

[13] Shamsipur M., Bahrami-Adeh N., Hajitarverdi M.S., Yazdimamaghani M., Zarei F., Influence of Micro and Nano Silica on Mechanical Properties of Plasticized Sulfur Composites, *Iran. J. Chem. Chem. Eng. (IJCCE)*, **32**(3): 1-7 (2013).

[14] Jahanmardi R., Kangarlou B., Ranjbarzadeh-Dibazar A., Effects of Organically Modified Nanoclay on Cellular Morphology, Tensile Properties, and Dimensional Stability of Flexible Polyurethane Foams, *J. Nanostruct. Chem.*, **3**:82 (2013).

[15] Lee L.J., Zeng C., Cao X., Han X., Shen J., Xu G., Polymer Nanocomposite Foams, *Compos. Sci. Technol.*, **65**(15-16): 2344-2363 (2005).

[16] Arab-Baraghi M., Mohammadizadeh M., Jahanmardi R., A simple method for Preparation of Polymer Microcellular Foams by In-Situ Generation of Supercritical Carbon Dioxide From Dry Ice, *Iran. Polym. J.*, **23**(6): 427-435 (2014).

[17] Ahmadi M., Jahanmardi R., Mohammadizadeh M., Preparation of PMMA/MWNTs Nanocomposite Microcellular Foams by In-situ Generation of Supercritical Carbon Dioxide, *Iran. J. Chem. Chem. Eng. (IJCCE)*, **35**(2): 63-72 (2016).

[18] Alveraz P., Mendizabal A., Petite M., Rodriguez-Perez M.A., Echeverria A., Finite Element Modeling of Compressive Mechanical Behaviour of High and Low Density Polymeric Foams, *Mat.-wiss. u. Werkstofftech.* **40**(3): 126-132 (2009).

[19] Colquhoun H.M., Chappell D., Lewis A.L., Lewis D.F., Finlan G.T., Williams P.J., Chlorine Tolerant, Multilayer Reverse-Osmosis Membranes with High Permeate Flux and High Salt Rejection, *J. Mater. Chem.*, **20**(22)**:** 4629-4634(2010).

[20] Tajeddin B., Ramedani.N., Preparation and Characterization (Mechanical and Water Absorption Properties) of CMC/PVA/Clay Nanocomposite Films, *Iran. J. Chem. Chem. Eng. (IJCCE)*, **35**(3): 9-15 (2016).

[21] Mallakpour S., Dinari M., Synthesis and Properties of Biodegradable Poly(vinyl alcohol)/Organo-nanoclay Bionanocomposites, *J. Polym. Environ.*, **20**(3): 732-740 (2012).